Available online at www.sciencedirect.com
ScienceDirect
Trans. Nonferrous Met. Soc. China 23(2013) 756−764
Transactions of Nonferrous Metals Society of China
www.tnmsc.cn

Hot deformation behavior and processing maps of Mg−Zn−Cu−Zr magnesium alloy

Hui YU[1,2], Hua-shun YU[1], Young-min KIM[2], Bong-sun YOU[2], Guang-hui MIN[1]

1. Key Laboratory for Liquid−Solid Evolution and Processing of Materials, Ministry of Education, School of Materials Science and Engineering Shandong University, Ji'nan 250061, China;
2. Light Metals Group, Korea Institute of Materials Science, Changwon 642831, Korea

Received 21 May 2012; accepted 5 November 2012

Abstract: The deformation behaviors of a new quaternary Mg−6Zn−1.5Cu−0.5Zr alloy at temperatures of 523−673 K and strain rates of 0.001−1 s^{-1} were studied by compressive tests using a Gleeble 3800 thermal-simulator. The results show that the flow stress increases as the deformation temperature decreases or as the strain rate increases. A strain-dependent constitutive equation and a feed-forward back-propagation artificial neural network were used to predict flow stress, which showed good agreement with experimental data. The processing map suggests that the domains of 643−673 K and 0.001−0.01 s^{-1} are corresponded to optimum conditions for hot working of the T4-treated Mg−6Zn−1.5Cu−0.5Zr alloy.

Key words: Mg alloy; Cu addition; flow stress; deformation behavior; constitutive equation; artificial neural network; processing map

1 Introduction

As the lightest metallic structural materials, magnesium and its alloys recently show the most promising development due to their low density, high specific strength and specific stiffness, good damping capacity, excellent machinability and high recycling rate. Accordingly, Mg alloys have great potential in the aerospace, aircraft and automobile industries [1].

Copper (Cu) is cost-effective, compared with some rare earth elements such as Ce, Nd, Y and Gd. According to reports by ZHU et al [2] and BUHA and OHKUBO [3], Mg−Zn−Cu alloys (ZC series) that have good castability show a significant increase in age-hardening response compared with binary Mg−Zn alloy. As Cu addition can increase eutectic temperatures, Cu-added alloys can be solution-treated at higher temperatures. The addition of minor alloying elements such as Mn, Al, Zr to Mg−Zn−Cu alloys can make significant influences on mechanical properties; for instance, a favorable combination of high ductility, yield strength and hardness can be achieved in naturally-aged cast Mg−6Zn−2Cu−0.1Mn alloy [4]. Zirconium (Zr) can significantly refine grain size of cast products, resulting in improving tensile properties and corrosion resistance [5].

Meanwhile, designers of metal forming process are eager to understand how metals and alloys behave under certain hot-working conditions. The constitutive equation is a powerful tool which can describe the plastic flow behaviors of metals and alloys. Based on the principle of the dynamic material model (DMM), processing maps are constructed to figure out the optimum conditions for hot working processes [6]. Although many researchers have attempted to utilize these tools with a wide range of materials including Mg−Zn−Zr and Mg−Al−Zn alloys [1,7−13], there have been rare studies on the hot deformation behavior and workability of Mg−Zn−Cu−Zr magnesium alloy. In this study, therefore, we investigated the plastic flow behaviors of Mg−6Zn−1.5Cu−0.5Zr magnesium alloy. Two approaches (regression and artificial neural network) were used to develop the strain-dependent models to predict the flow stress. In addition, the processing maps of Mg−6Zn−1.5Cu−0.5Zr magnesium alloy at different strain levels were constructed to determine the optimum conditions for hot working process, using the calculated strain-rate sensitivity.

Corresponding author: Young-min KIM; Tel: +82-55-2803537; Fax: +82-55-2803599; E-mail: ymkim@kims.re.kr
DOI: 10.1016/S1003-6326(13)62526-1

2 Experimental

The nominal composition of the studied alloy is Mg−6%Zn−1.5%Cu−0.5%Zr (referred as ZCK620). The alloy was prepared by a permanent mold casting method at 993 K under a protective mixture of CO_2 and SF_6 atmosphere. The composition of the billet (100 mm in diameter and 200 mm in length) was measured using an inductively coupled plasma spectrometer, which was very close to the nominal value. The billet was homogenized at 673 K for 8 h. Cylindrical specimens (8 mm in diameter and 12 mm in length) were machined from the homogenized billet. Hot compressive tests were conducted with a Gleeble 3800 thermo-simulator at a temperature range of 523−673 K and interval of 50 K. Four typical strain rates were selected from 0.001 to 1 s^{-1}. The temperature was controlled and measured with a thermocouple welded to the mid-height of the sample. All specimens were heated at 10 K/s up to deformation temperature, held for 5 min to homogenize the temperature of the sample, and then deformed up to a true strain of 0.8. A three-layer feed-forward back-propagation ANN with Levenberg-Marquardt learning algorithm was used to predict the flow stress, and then compared with those calculated by the regression method.

3 Results and discussion

3.1 True stress—true train curves

The true stress—true strain curves of the ZCK620 magnesium alloy obtained at different strain rates are shown in Fig. 1. Generally, the flow stress increases to a peak and then decreases to a steady state. For instance, the curve at strain rate of 1 s^{-1} shows a hardening stage, a softening stage, and a steady stage. The different stages come from the combined effects of work hardening (WH), dynamic recovery (DRV) as well as dynamic recrystallization (DRX) [14]. In addition, the flow stress increases as the deformation temperature decreases or as the strain rate increases.

3.2 Strain-dependent constitutive equation

The relationship between the flow stress, the strain rate, and the temperature is commonly expressed as follows [14−17]:

$$\dot{\varepsilon} = A_1 \sigma^{n_1} \quad (1)$$

$$\dot{\varepsilon} = A_2 \exp(\beta\sigma) \quad (2)$$

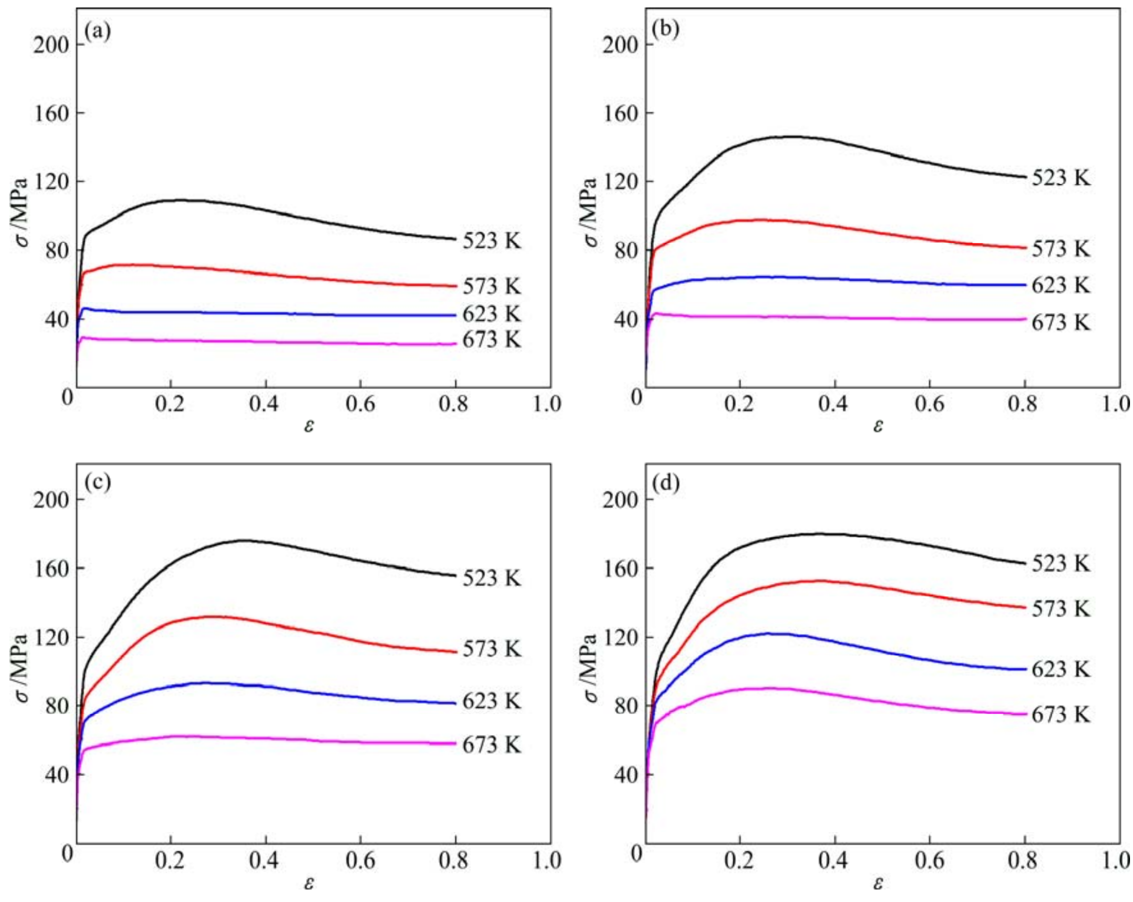

Fig. 1 True stress—true strain curves of ZCK620 magnesium alloy at various temperatures with different strain rates: (a) $\dot{\varepsilon}$=0.001 s^{-1}; (b) $\dot{\varepsilon}$=0.01 s^{-1}; (c) $\dot{\varepsilon}$=0.1 s^{-1}; (d) $\dot{\varepsilon}$=1 s^{-1}

$$\dot{\varepsilon} = A[\sinh(\alpha\sigma)]^n \exp\left(-\frac{Q}{RT}\right) \tag{3}$$

where n_1, A_1, β, A_2, A and α ($\alpha=\beta/n_1$) are material constants. Equations (1) and (2) are usually applied to low stress and high stress, respectively. Equation (3) in the hyperbolic sine law is generally used to describe the flow stress and deformation activation behavior over a wide range of temperature and strain rate. Q is the activation energy for deformation; R is the mole gas constant (8.314 J/mol K); σ is the flow stress; T is the temperature.

ZENER and HOLLOMON [18] proposed a flow stress model, where the relationship between temperature and strain rate is denoted by a parameter Z:

$$Z = \dot{\varepsilon} \exp\left(\frac{Q}{RT}\right) = A[\sinh(\alpha\sigma)]^n \tag{4}$$

Considering the definition of the hyperbolic law, the flow stress can be expressed as the function of the Zener-Hollomon parameter:

$$\sigma = \frac{1}{\alpha}\ln\left\{\left(\frac{Z}{A}\right)^{1/n} + \left[\left(\frac{Z}{A}\right)^{2/n} + 1\right]^{1/2}\right\} \tag{5}$$

Due to similar behavior of peak stress and steady-state stress, the constitution equation was calculated using the peak stress (σ_p). The value of n_1 and β can be obtained from the slopes of the $\ln\dot{\varepsilon}$—$\ln\sigma_p$ (Fig. 2(a)) and $\ln\dot{\varepsilon}$—σ_p (Fig. 2(b)) plots, respectively. The calculated mean values of n_1, β, and α ($=\beta/n_1$) are 6.636, 0.0904 MPa^{-1}, and 0.0136 MPa^{-1}, respectively. For a given strain rate, the activation energy Q can be calculated as follows:

$$Q = R\left.\frac{\partial \ln\dot{\varepsilon}}{\partial \ln[\sinh(\alpha\sigma)]}\right|_T \cdot \left.\frac{\partial \ln[\sinh(\alpha\sigma)]}{\partial(1/T)}\right|_{\dot{\varepsilon}} \tag{6}$$

Therefore, by substituting the values of temperature and peak flow stress, the value of Q can be obtained from the slope of the plots of $\ln\dot{\varepsilon}$ vs $\ln[\sinh(\alpha\sigma)]$ (Fig. 2(c)) and $\ln[\sinh(\alpha\sigma)]$ vs $1/T$ (Fig. 2(d)), respectively. The calculated Q value is 176.8293 kJ/mol. From the natural logarithm used in Eq. (4), the linear-relationship between $\ln[\sinh(\alpha\sigma)]$ and $\ln Z$ was obtained, as shown in Fig. 3. From the above results, the peak stress can be expressed by substituting Eq. (5) with the following parameters: α=0.0136 MPa^{-1}, $Z=\dot{\varepsilon}\exp[176829.3/(RT)]$, A=2.0926×10^{12}, and n=5.0692.

Then, the material constants (α, n, Q, $\ln A$) of the constitutive equations were computed under different deformation strains within the range of 0.05−0.8 at the interval of 0.05. The relationships between α, n, Q, $\ln A$ and true strain for ZCK620 magnesium alloy (Fig. 4) can

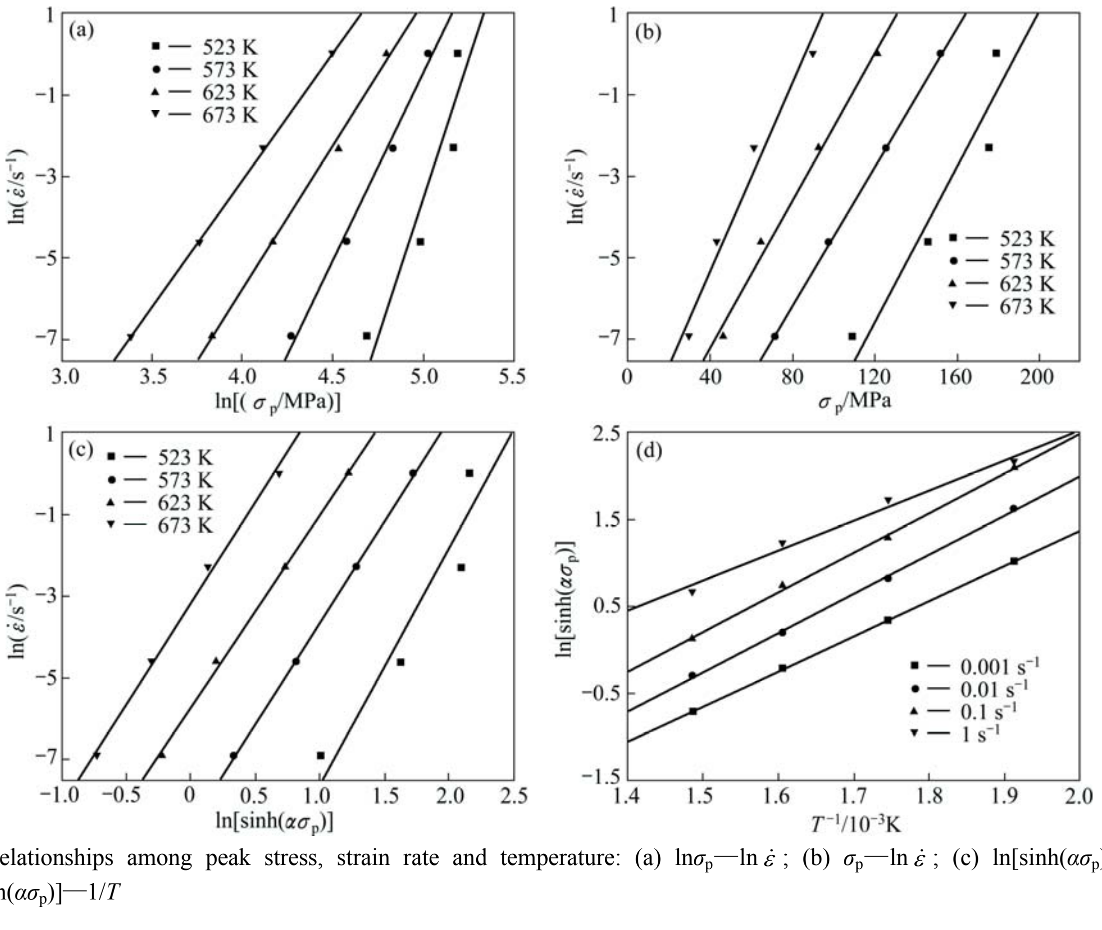

Fig. 2 Relationships among peak stress, strain rate and temperature: (a) $\ln\sigma_p$—$\ln\dot{\varepsilon}$; (b) σ_p—$\ln\dot{\varepsilon}$; (c) $\ln[\sinh(\alpha\sigma_p)]$—$\ln\dot{\varepsilon}$; (d) $\ln[\sinh(\alpha\sigma_p)]$—$1/T$

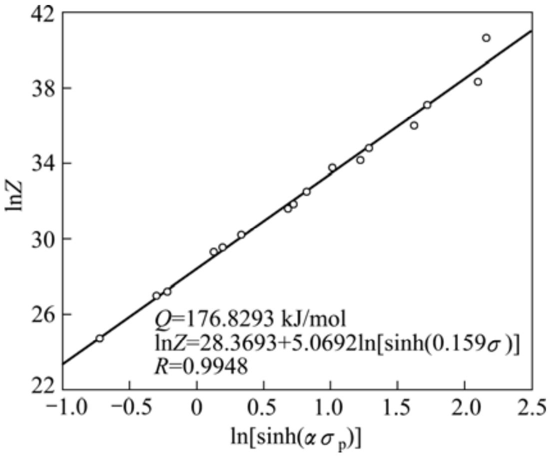

Fig. 3 Relationship between flow stress and Zener−Hollomon parameter

be fitted by the fifth-order polynomials.

$$\alpha = A_0 + A_1\varepsilon + A_2\varepsilon^2 + A_3\varepsilon^3 + A_4\varepsilon^4 + A_5\varepsilon^5 \tag{7}$$

$$n = B_0 + B_1\varepsilon + B_2\varepsilon^2 + B_3\varepsilon^3 + B_4\varepsilon^4 + B_5\varepsilon^5 \tag{8}$$

$$Q = C_0 + C_1\varepsilon + C_2\varepsilon^2 + C_3\varepsilon^3 + C_4\varepsilon^4 + C_5\varepsilon^5 \tag{9}$$

$$\ln A = D_0 + D_1\varepsilon + D_2\varepsilon^2 + D_3\varepsilon^3 + D_4\varepsilon^4 + D_5\varepsilon^5 \tag{10}$$

The α, n, Q, and ln A can be measured through the least square method, and they are summarized in Table 1.

Table 1 Results of α, n, Q, ln A of ZCK620 Mg alloy in polynomial fit

Equation	Parameter
Eq. (7)	A_0=0.0491, A_1=−0.373, A_2=1.6693, A_3=−3.6911, A_4=3.9299 A_5=−1.6022
Eq. (8)	B_0=5.3119, B_1=−3.0863, B_2=−4.5364, B_3=56.2357, B_4=−95.1206, B_5=48.3322
Eq. (9)	C_0=250.017, C_1=−860.9199, C_2=3583.5383, C_3=−7355.0188, C_4=7325.7735, C_5=−2838.0401
Eq. (10)	D_0=32.1887, D_1=−53.8861, D_2=199.0253, D_3=−322.3007, D_4=238.9525, D_5=68.3331,

In addition, four kinds of standard statistical performance evaluation methods were used to evaluate the accuracy of the developed constitutive equation, namely, the correlation coefficient (R), the average absolute relative error (E), the relative error (δ) and the standard deviation (S.D.). They are expressed as follows:

$$R = \frac{\sum_{i=1}^{n}(E_i - \overline{E})(P_i - \overline{P})}{\sqrt{\sum_{i=1}^{n}(E_i - \overline{E})^2 \sum_{i=1}^{n}(P_i - \overline{P})^2}} \tag{11}$$

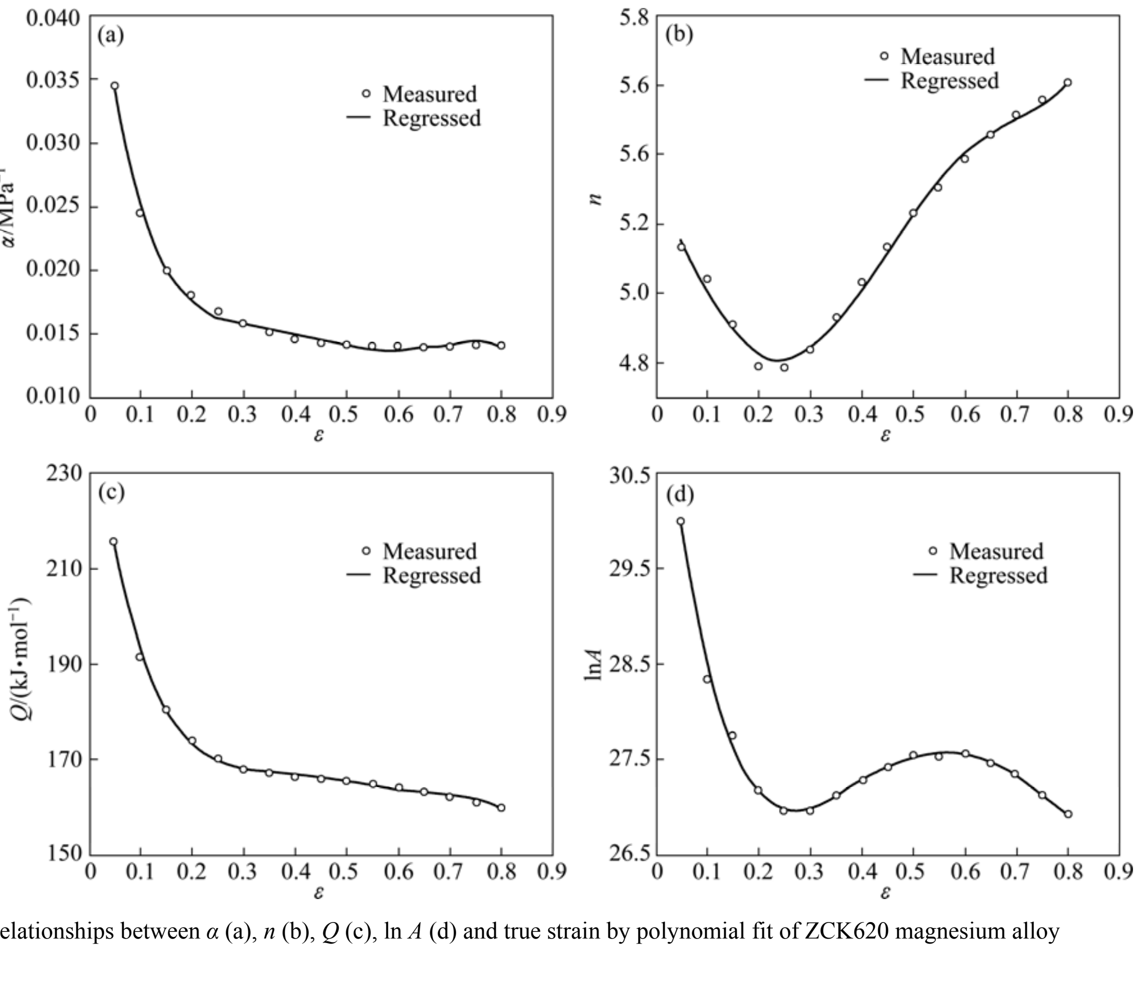

Fig. 4 Relationships between α (a), n (b), Q (c), ln A (d) and true strain by polynomial fit of ZCK620 magnesium alloy

$$E=\frac{1}{n}\sum_{i=1}^{n}\left|\frac{E_i-P_i}{E_i}\right|\times 100\% \quad (12)$$

$$\delta=\left(\frac{E_i-P_i}{E_i}\right)\times 100\% \quad (13)$$

$$\text{S.D.}=\sqrt{\frac{\sum_{i=1}^{n}(X_i-\overline{X})^2}{n-1}} \quad (14)$$

where E_i and P_i are experimental and predicted values, respectively; $\overline{E}$ and $\overline{P}$ are the mean values of E_i and P_i, respectively; X and $\overline{X}$ are the original data and mean value of X, respectively; N is the total number employed in this study. As shown in Figs. 5(a) and (a′), the experimental and predicted results show a good agreement.

3.3 Artificial neural network model

In the regression method, however, the response of the deformation behaviors of the materials under elevated temperatures and increased strain rates is highly nonlinear, and many factors affecting the flow stress are also nonlinear, which make the accuracy of the flow stress predicted by the regression methods lower and the applicable range limited [19]. In most cases, one hidden layer is found to be adequate, and this reaffirms the universal approximation theorem that a single layer of non-linear hidden units is sufficient to approximate any continuous function [20]. In this study, we determined the optimal number of neurons in the hidden layer by comparing the performance of the network, with 7−20 hidden neurons, and found that 8 neurons produced the greatest network performance. The schematic diagram of

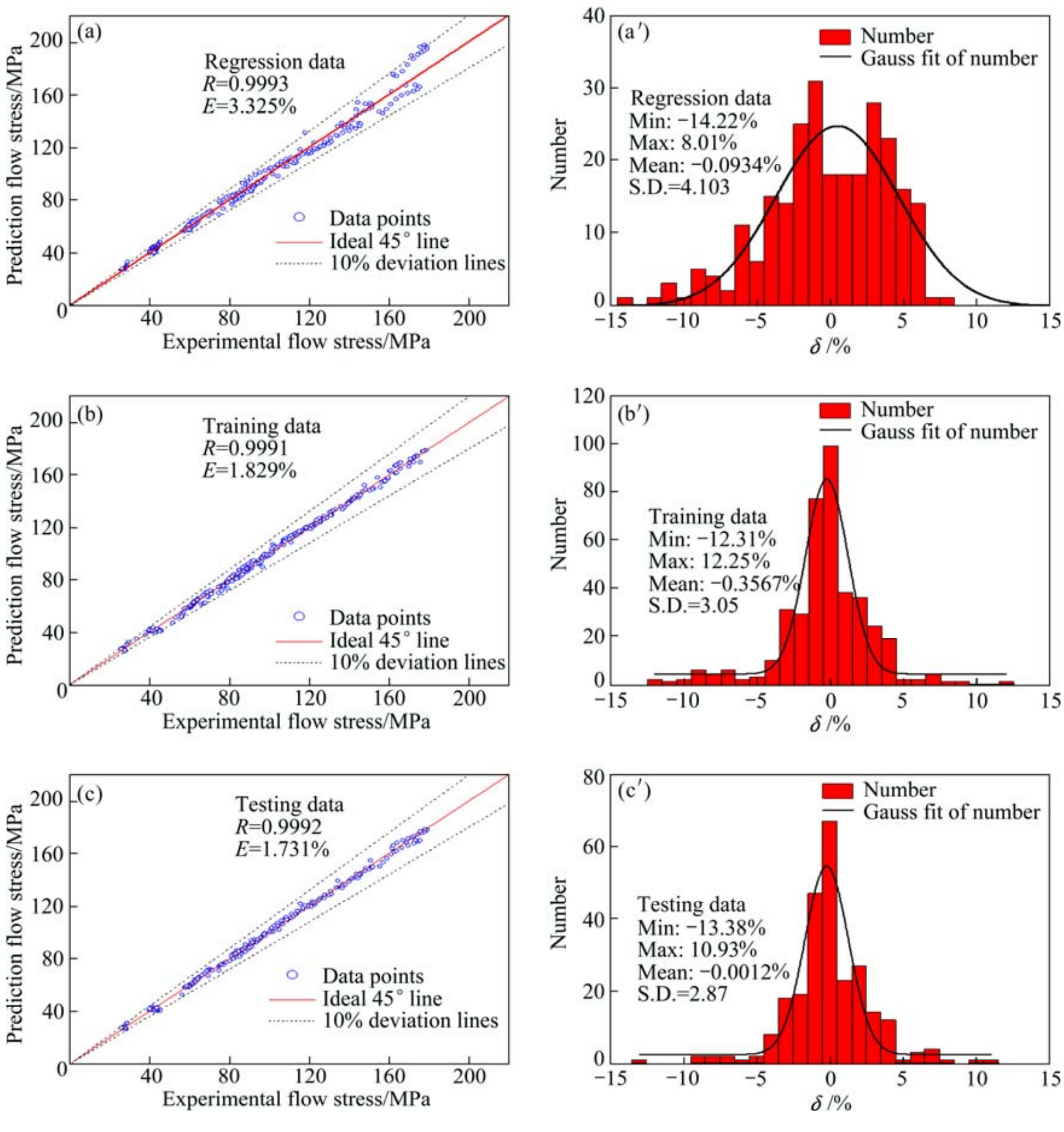

Fig. 5 Comparison between experimental and predicted flow stress of ZCK620 magnesium alloy using ANN: (a) Regression data; (b) Training data; (c) Testing data; (a′), (b′), (c′) Corresponding statistical analyses of relative error of (a), (b), (c), respectively

the ANN structure for flow stress prediction of the ZCK620 alloy is shown in Fig. 6. The inputs of the network are temperature (T), strain rate ($\dot{\varepsilon}$), and strain (ε), respectively, and stress (σ) is the output. A total of 656 input-output data were selected from the true stress—true strain curves. The 256 points at true strains between 0.05 and 0.8 with interval of 0.05 were chosen to test the predictability of ANN model, while the remaining 400 points were used to train. Before the training of the network, both input and output variables were normalized with the range of 0−1 as follows:

$$X' = 0.1 + 0.8 \times \left(\frac{X - X_{\min}}{X_{\max} - X_{\min}} \right) \tag{15}$$

where X' is the normalized value of a certain parameter (T, ε, σ); X is the measured value for this parameter; $X_{\min}$ and $X_{\max}$ are the minimum and the maximum values for this parameter, respectively. Since $\dot{\varepsilon}$ often changes by an order of magnitude, the following logarithm equation is adopted to normalize:

$$\dot{\varepsilon}' = 0.1 + 0.8 \times \left(\frac{\ln \dot{\varepsilon} - \ln \dot{\varepsilon}_{\min}}{\ln \dot{\varepsilon}_{\max} - \ln \dot{\varepsilon}_{\min}} \right) \tag{16}$$

The results of the statistical analyses of the variables used to develop the ANN model for ZCK620 magnesium alloy are listed in Table 2.

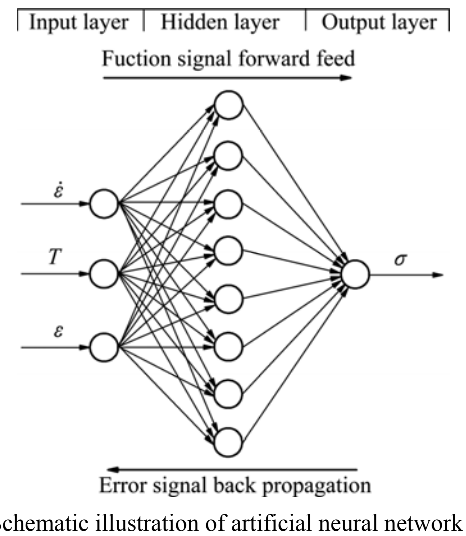

Fig. 6 Schematic illustration of artificial neural network

Table 2 Statistical analysis of variables used to develop ANN model

Variable	Minimum value	Maximum value	Average	Standard deviation
$\dot{\varepsilon}$ /s^{-1}	0.001	1	0.2848	0.4249
T/K	523	673	598.9909	56.0718
ε	0.0036	0.8009	0.3855	0.2334
σ/MPa	25.6378	179.214	91.7104	41.4517

After training and testing, the neural network performance was checked as shown in Figs. 5(b) and (c). The diagrams show an analysis of the network response in a form of linear regression analysis between the network outputs (predicted data) and the corresponding targets (experimental data). It is obvious that the predicted values from the trained neural network outputs track the targets very well. Additionally, we calculated the δ of neural network (Figs. 5(b′) and (c′)), and the δ showed a typical Gaussian distribution with the mean value at about zero.

As shown in Fig. 7, the effects of deformation temperature and strain rate on the flow behaviors of ZCK620 magnesium alloy are simulated using the developed ANN model. Obviously, the predicted results agreed well with the experimental data. Both the deformation temperature and strain rate have pronounced influences on the flow stress. The flow stress decreases with an increase in deformation temperature and a decrease in strain rate, which can be explained by the terms of dynamic recrystallization and dislocation mechanism [19,21].

3.4 Processing map

In DMM, the work piece is considered to be a dissipater of power and the characteristics of power dissipation through microstructural changes are expressed in terms of an efficiency of power dissipation given by $\eta=2m/(m+1)$, where m ($\partial(\ln\sigma)/\partial\ln(\dot{\varepsilon})$) is the strain rate sensitivity of flow stress.

According to the criterion developed in Refs. [1,6, 13], flow instability will occur if

$$\xi(\dot{\varepsilon}) = \left\{ \frac{\partial \ln[m/(m+1)]}{\partial \ln(\dot{\varepsilon})} \right\} + m < 0 \tag{17}$$

Figures 8 (a)−(d) present the processing maps of T4-treated ZCK620 magnesium alloy at different strains. The processing map is superimposed by the instability map on the power dissipation map, the contour represents constant efficiency (in percentage), and the gray areas indicate the regimes of flow instability. The strain levels of 0.1, 0.3, 0.5, and 0.8 correspond to the pre-peak strain, the peak strain, the post-peak strain, and the steady-state strain, respectively. It is obvious that the strain level has a significant effect on the processing maps. As the strain increases, the region with a low temperature and a low strain rate changes to a region with a low temperature and a medium strain rate, and a region with a medium-high temperature and a high strain rate. In the instable region, the efficiency of the power dissipation decreases rapidly, which should be avoided for hot working processes. In addition, the optimum parameters for subsequent processing have been suggested at the peak efficiency, where the dynamic

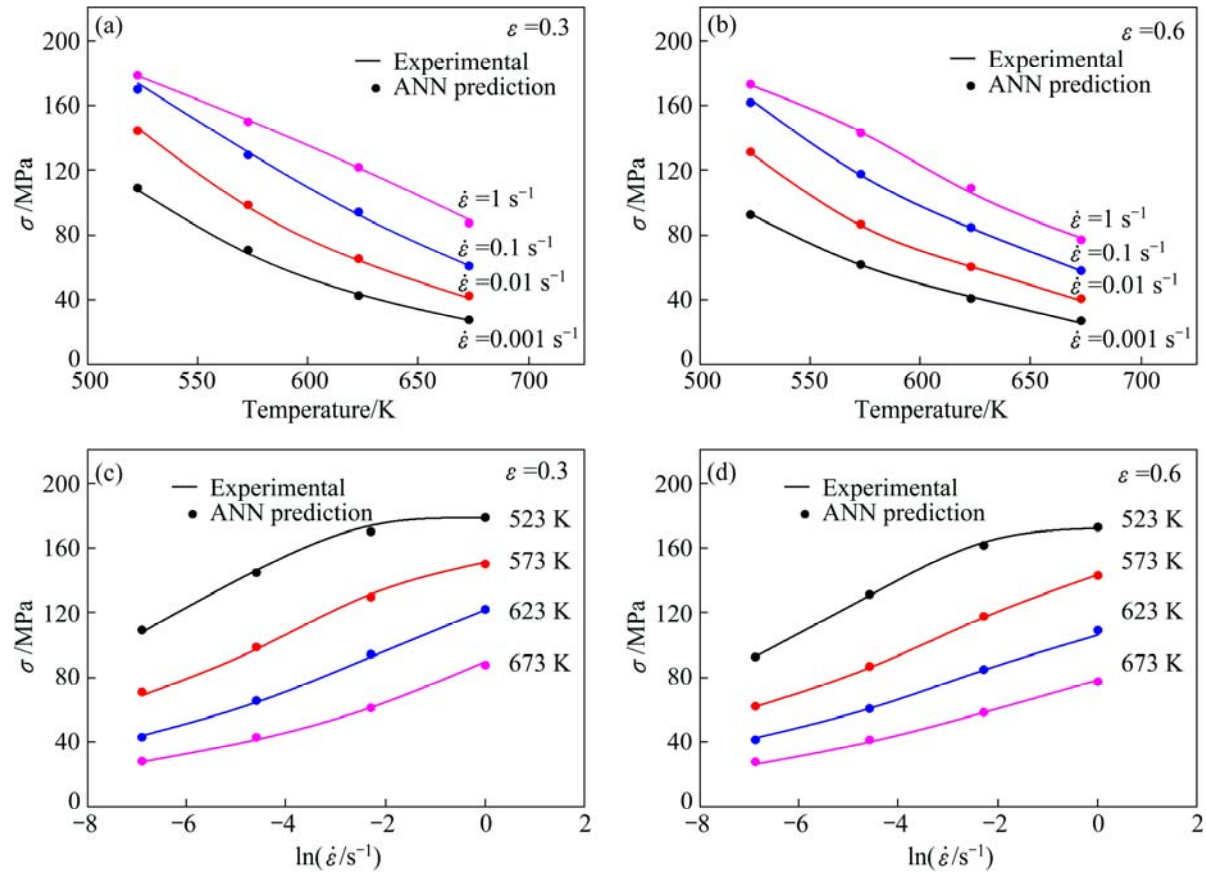

Fig. 7 Comparisons between experimental and predicted flow stress of ZCK620 magnesium alloy using ANN at different strains: (a, b) effects of deformation temperature; (c, d) Effects of strain rate

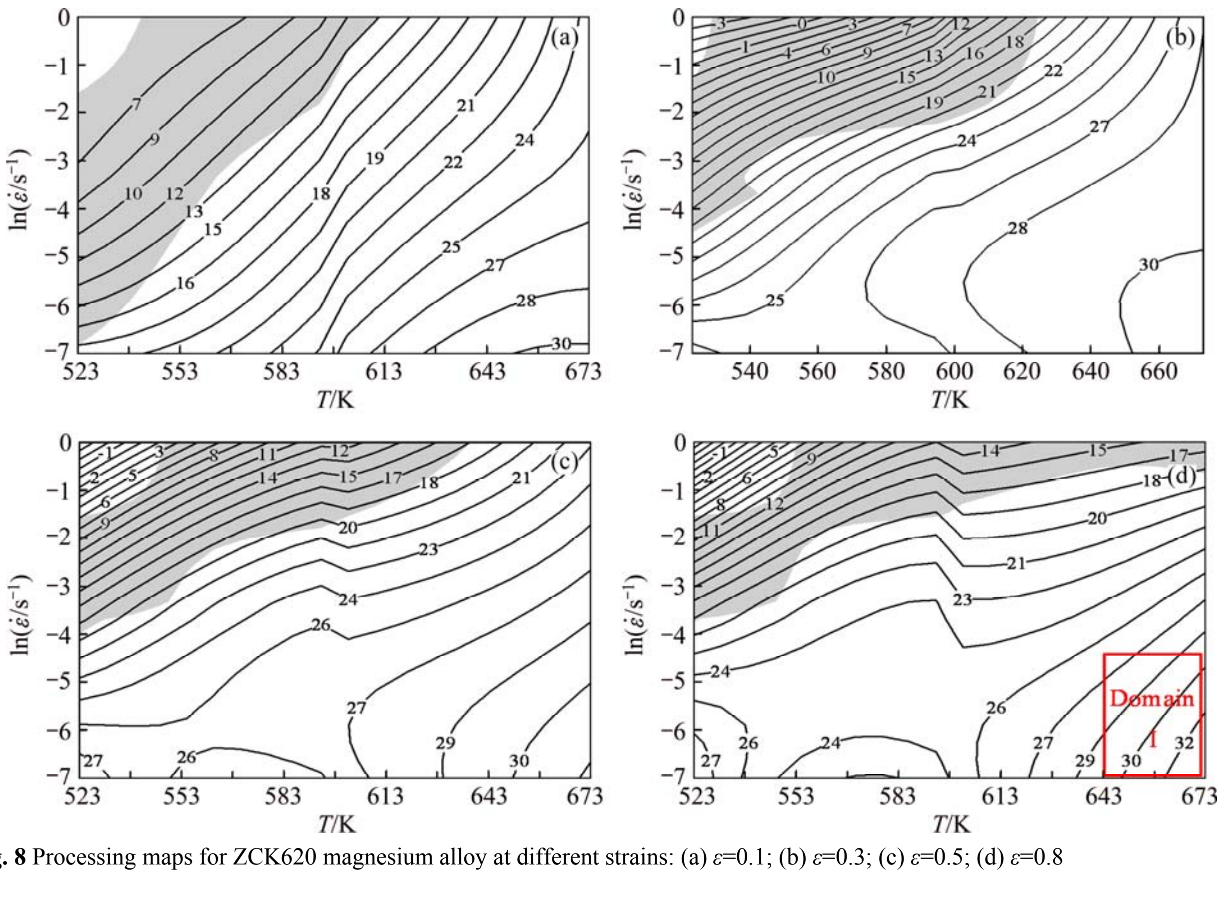

Fig. 8 Processing maps for ZCK620 magnesium alloy at different strains: (a) ε=0.1; (b) ε=0.3; (c) ε=0.5; (d) ε=0.8

recrystallization is operating to reduce the tendency for flow localization [13]. Thus, the optimized condition to conduct the hot working is Domain I (temperature range of 643−673 K and strain rate range of 10^{-3}–10^{-2} s^{-1}) for ZCK620 magnesium alloy.

4 Conclusions

1) A strain-dependent constitutive equation and a feed-forward back-propagation artificial neural network are developed to predict the flow stress for the entire strain range. Good agreements between the experimentally measured values and the calculated ones of the flow stress are observed in both of the models.

2) A comparison of the results of predicting the flow stress using the regression and the ANN model shows that the latter provides better agreement with the experimentally measured data.

3) According strain-dependent constitutive analysis using the ANN model, processing maps of the ZCK620 alloy at different strain levels were constructed. The optimum processing conditions for hot working of the ZCK620 alloy are in the range of 643−673 K and 0.001−0.01 s^{-1}.

Acknowledgements

This study was financially supported by the R&D Program of Korea Institute of Materials Science and the World Premier Materials Program funded by The Ministry of Knowledge Economy, Korea. One of the authors (Hui YU) is grateful for the financial support from China Scholarship Council (CSC) and Dr. Chao ZHENG for ANN discussion.

References

[1] WANG C Y, WANG X J, CHANG H, WU K, ZHENG M Y. Processing maps for hot working of ZK60 magnesium alloy [J]. Materials Science and Engineering A, 2007, 464(1−2): 52−58.

[2] ZHU H M, SHA G, LIU J W, WU C L, LUO C P, LIU Z W, ZHENG P K, RINGER S P. Microstructure and mechanical properties of Mg−6Zn−*x*Cu−0.6Zr (wt.%) alloys [J]. Journal of Alloys and Compounds, 2011, 509(8): 3526−3531.

[3] BUHA J, OHKUBO T. Natural aging in Mg−Zn(−Cu) alloys [J]. Metallurgical and Materials Transactions A, 2008, 39(9): 2259−2273.

[4] BUHA J. Mechanical properties of naturally aged Mg−Zn−Cu−Mn alloy [J]. Materials Science and Engineering A, 2008, 489(1−2): 127−137.

[5] SUN M, WU G, WANG W, DING W. Effect of Zr on the microstructure, mechanical properties and corrosion resistance of Mg−10Gd−3Y magnesium alloy [J]. Materials Science and Engineering A, 2009, 523(1−2): 145−151.

[6] PRASAD Y V R K. Processing maps: A status report [J]. Journal of Materials Engineering and Performance, 2003, 12(6): 638−645.

[7] GALIYEV A, KAIBYSHEV R, GOTTSTEIN G. Correlation of plastic deformation and dynamic recrystallization in magnesium alloy ZK60 [J]. Acta Materialia, 2001, 49(7): 1199−1207.

[8] MCQUEEN H J, RYAN N D. Constitutive analysis in hot working [J]. Materials Science and Engineering A, 2002, 322(1−2): 43−63.

[9] SLOOFF F A, ZHOU J, DUSZCZYK J, KATGERMAN L. Strain-dependent constitutive analysis of three wrought Mg−Al−Zn alloys [J]. Journal of Materials Science, 2008, 43(22): 7165−7170.

[10] QUAN G Z, KU T W, SONG W J, KANG B S. The workability evaluation of wrought AZ80 magnesium alloy in hot compression [J]. Materials & Design, 2011, 32(4): 2462−2468.

[11] ROBI P S, DIXIT U S. Application of neural networks in generating processing map for hot working [J]. Journal of Materials Processing Technology, 2003, 142(1): 289−294.

[12] SRINIVASAN N, PRASAD Y V R K, RAO P R. Hot deformation behavior of Mg−3Al alloy—A study using processing map [J]. Materials Science and Engineering A, 2008, 476(1−2): 146−156.

[13] ZHOU H T, LI Q B, ZHAO Z K, LIU Z C, WEN S F, WANG Q D. Hot workability characteristics of magnesium alloy AZ80−A study using processing map [J]. Materials Science and Engineering A, 2010, 527(7−8): 2022−2066.

[14] QIN Y, PAN Q, HE Y, LI W, LIU X, FAN X. Modeling of flow stress considering dynamic recrystallization for magnesium alloy ZK60 [J]. Materials and Manufacturing Processes, 2010, 25: 527−533.

[15] LIN Y C, CHEN M S, ZHONG J. Constitutive modeling for elevated temperature flow behavior of 42CrMo steel [J]. Computational Materials Science, 2008, 42(3): 470−477.

[16] SLOFF F A, ZHOU J, DUSZCZYK J, KATGERMAN L. Constitutive analysis of wrought magnesium alloy Mg−Al4−Zn1 [J]. Scripta Materialia, 2007, 57(8): 759−762.

[17] YANG Z, GUO Y C, LI J P, HE F, XIA F, LIANG M X. Plastic deformation and dynamic recrystallization behaviors of Mg−5Gd−4Y−0.5Zn−0.5Zr alloy [J]. Materials Science and Engineering A, 2008, 485(1−2): 487−491.

[18] ZENER C, HOLLOMON J H. Effect of strain rate upon plastic flow of steel [J]. Journal of Applied Physics, 1944, 15: 22−32.

[19] QIN Y J, PAN Q L, HE Y B, LI W B, LIU X Y, FAN X. Artificial neural network modeling to evaluate and predict the deformation behavior of ZK60 magnesium alloy during hot compression [J]. Materials and Manufacturing Processes, 2010, 25(7): 539−545.

[20] MANDAL S, SIVAPRASAD P V, VENUGOPL S, MURTHY K P N, RAJ B. Artificial neural network modeling of composition-process-property correlations in austenitic stainless steels [J]. Materials Science and Engineering A, 2008, 485(1−2): 571−580.

[21] LIN Y C, ZHANG J, ZHONG J. Application of neural networks to predict the elevated temperature flow behavior of a low alloy steel [J]. Computational Materials Science, 2008, 43(4): 752−758.

Mg−Zn−Cu−Zr 镁合金的热变形行为和加工图

余 晖[1,2], 于化顺[1], Young-min KIM[2], Bong-sun YOU[2], 闵光辉[1]

1. 山东大学 材料科学与工程学院，材料液固结构演变与加工教育部重点实验室，济南 250061；
2. Light Metals Group, Korea Institute of Materials Science, Changwon 642831, Korea

摘　要：在温度 523~673 K，应变率 0.001~1 s^{-1} 条件下，使用 Gleeble 3800 热模拟机研究一种新的四元 Mg−6Zn−1.5Cu−0.5Zr 合金的变形行为。结果表明，流变应力随着变形温度的升高或随着应变率的下降而减小。采用依赖于应变的本构方程和前馈反向传播人工神经网络来预测流变应力，其结果与实验数据吻合很好。热加工图表明，对于经 T4 处理的 Mg−6Zn−1.5Cu−0.5Zr 合金的热加工，其最佳工作条件为温度 643~673 K，应变速率 0.001~0.01 s^{-1}。

关键词：镁合金；铜添加；流变应力；变形行为；本构方程；人工神经网络；加工图

(Edited by Xiang-qun LI)